frontiers | Frontiers in Earth Science

TYPE Original Research
PUBLISHED 29 August 2022
DOI 10.3389/feart.2022.928115

Check for updates

OPEN ACCESS

EDITED BY
Patrick G. Hatcher,
Old Dominion University, United States

REVIEWED BY
Kelly Gibson,
University of South Carolina Aiken, United States
Rong Xiang,
South China Sea Institute of Oceanology, China

*CORRESPONDENCE
Hon-Kit Lui,
hklui@mail.nsysu.edu.tw

SPECIALTY SECTION
This article was submitted to Biogeoscience, a section of the journal Frontiers in Earth Science

RECEIVED 25 April 2022
ACCEPTED 29 July 2022
PUBLISHED 29 August 2022

CITATION
Lin H-L, Lui H-K, Lin T-C and Wang Y-L (2022), Response of planktonic foraminifera to seasonal and interannual hydrographic changes: Sediment trap record from the northern South China Sea.
Front. Earth Sci. 10:928115.
doi: 10.3389/feart.2022.928115

COPYRIGHT
© 2022 Lin, Lui, Lin and Wang. This is an open-access article distributed under the terms of the Creative Commons Attribution License (CC BY). The use, distribution or reproduction in other forums is permitted, provided the original author(s) and the copyright owner(s) are credited and that the original publication in this journal is cited, in accordance with accepted academic practice. No use, distribution or reproduction is permitted which does not comply with these terms.

Response of planktonic foraminifera to seasonal and interannual hydrographic changes: Sediment trap record from the northern South China Sea

Hui-Ling Lin[1], Hon-Kit Lui[1]*, Tai-Chun Lin[1] and You-Lin Wang[2]

[1]Department of Oceanography, National Sun Yat-Sen University, Kaohsiung, Taiwan, [2]Department of Earth Sciences, National Taiwan Normal University, Taipei, Taiwan

Foraminifera play an important role in the organic and inorganic carbon pumps of the ocean. Understanding their responses in seasonal and interannual time scales to the climate and seawater chemistry changes is important for studying carbon cycles and paleoclimatology. This study examined about 5.1-year continuous mass fluxes in 2013/9-2019/8 and 1.8-year planktonic foraminiferal shell fluxes in 2016/8-2019/8 census from ten and four sets of sediment traps, respectively, moored at the South East Asia Time-series Study (SEATS) site in the northern South China Sea (SCS), the world's largest marginal sea. A total of four sets of sediment trap mooring with 11 common species were identified, spanning from August 2016 to August 2019 with 8-day and 16-day collecting periods, which provided access to evaluate the impact of the prevailing monsoon system and interannual climatic conditions. Our results show that the winter monsoon enhances the nutrient inventories in the euphotic zone, supporting the productivity and the mass and shell fluxes. In addition to seasonal cycles, the variation of chlorophyll-*a* concentration in the SCS shows a strong response to wind speed under the influence of El Niño–Southern Oscillation (ENSO). The reduction in wind speed and the intensification of Kuroshio intrusion during the ENSO warm phases reduces the productivity and mass and shell fluxes, and vice versa in the case of the ENSO cold phases. The imprint of an ENSO cold phase (La Niña event) in 2017 was signified by 2–3-fold higher values than the 3-year average of total mass and foraminiferal shell fluxes. Instead of the common dominance of *Trilobatus sacculifer* and *Globigerinoides ruber* among species composition, *Neogloboquadrina dutertrei* was the predominant species comprising over 40%–60% of total shells greater than 212 μm. Furthermore, the interval with an elevated abundance of *N. dutertrei* lasted throughout January 2018 (four collecting intervals). Foraminifera shell fluxes were the lowest during warm months (March-August) in 2019, which was coeval with the increase in proportions of *Orbulina universa* and *Globigerinella calida*. The unusual species composition might signify a weak ENSO warm phase (A weak El Niño event) between September 2018 and August 2019.

KEYWORDS

sediment trap, planktonic foraminifera, South China Sea, ENSO, sinking particle, Kuroshio, West Philippine Sea, climate change

1 Introduction

Foraminifera are one of the key species that play an important role in the biological pump in the ocean. Reconstruction of paleoceanography relies on many proxy indicators generated from foraminifera preserved in marine sediments, including faunal census (Kipp et al., 1976; Niebler and Gersonde, 1998), stable isotopes $\delta^{13}C$ and $\delta^{18}O$ (Fairbanks et al., 1980; Fairbanks et al., 1982; Curry et al., 1983; Bouvier-Soumagnac and Duplessy, 1985; Spero and Lea, 1993, 1996; Spero et al., 1997; Gussone et al., 2003; Pogge von Strandmann, 2008), and trace elements (Nürnberg et al., 2000; Rosenthal et al., 2004; Yu et al., 2007; Mathien-Blard and Bassinot, 2009; Rae et al., 2011; Wu et al., 2015; Mezger et al., 2016; Bertlich et al., 2018; Mezger et al., 2018; Duhamel et al., 2020; Holland et al., 2020) of their shells. Knowing the life cycles and the abundances of different species helps interpreting the downcore records better. Truthful interpretation of downcore records, however, depends on a statistical correlation between modern foraminifera and the surrounding hydrographic changes. Additionally, understanding how different species of foraminifera respond to the climate and seawater chemistry changes is critical for predicting the changes in biological carbon cycles under global environment changes. Observations of living planktonic foraminifera have been achieved in the laboratory (Spero, 1992; Sanyal et al., 1996; Bijma et al., 1999; Bemis et al., 2000; Hönisch et al., 2003; Russell et al., 2004) and field studies, including plankton tows and sediment traps (Ravelo and Fairbanks, 1992; Black et al., 2001; Mulitza et al., 2003; Tedesco and Thunell, 2003; Kuroyanagi and Kawahata, 2004; Lin and Hsieh, 2007; Chapman, 2010; Lin et al., 2011; Lin, 2014; Jonkers et al., 2015; An et al., 2018; Ladigbolu et al., 2020). Although the ecological preferences and seasonality of popular species applied in paleoceanography have been well-documented to benefit from the continuous collection of sinking shells by sediment trap moorings (Black et al., 2001; Chapman, 2010; Lin et al., 2011; Sagawa et al., 2013; Lin, 2014; Jonkers et al., 2015), the response of modern planktonic foraminifera to interannual oscillation remains unclear.

Long-term time-series studies at regions with significant seasonal and interannual hydrographic oscillations are needed to examine the response of the vertical fluxes of foraminifera. Being situated between the Eurasia supercontinent and the immense Pacific Ocean, the meteorological forcing over the South China Sea (SCS), the world's largest marginal sea, is dominated by the East Asian Monsoon (Wu and Zhang, 1998; Liu et al., 2013). The East Asian Monsoon is one of the crucial factors governing the seasonal changes in hydrology and biogeochemistry in the northern SCS (nSCS) (Tseng et al., 2005; Wong et al., 2015). For instance, the wind-induced mixing increases nutrient inventory and productivity in the nSCS, causing higher productivity in the winter than in summer (Tseng et al., 2009a; Tseng et al., 2009b; Liu et al., 2013; Wong et al., 2015). The winter monsoon also intensifies the intrusion of high salinity but low nutrient Kuroshio into the nSCS. Of note, the El Niño–Southern Oscillation (ENSO) warm phases intensify the amount of Kuroshio intrusion into the SCS (Liu et al., 2013; Nan et al., 2013; Wu, 2013; Nan et al., 2015; Lui et al., 2020). Furthermore, the winter monsoon also brings terrestrial materials to the SCS in the form of dust, enhancing the flux of sinking particles (Ren et al., 2017; Du et al., 2021; Liao et al., 2021). Such backgrounds make the SCS a feasible area to examine the responses of foraminifera to the climate and seawater chemistry changes in seasonal and interannual time scales.

A time-series station, the South East Asia Time-series Study (SEATS) station, was established in 1998 in the nSCS as a part of the time series study in the Joint Global Ocean Flux Study (JGOFS, 1987–2003) (Chou et al., 2005; Tseng et al., 2005; Wong et al., 2007). The site was initially to the west of the Luzon Strait (around 18–19.5°N, 118.5°E) and was then relocated to the deep basin of the nSCS around 18°N, 116°E in 1999 (Figure 1). The major tasks of SEATS include seawater sampling at various depths and sinking particles collecting at depths of either 1,000 m and 3,500 m or 2,000 m and 3,500 m. Generally speaking, the Kuroshio is composed of the West Philippine Sea (WPS) and SCS water masses, with more SCS water on the left-hand side and more WPS water on the right-hand side (Chen et al., 2016). Mainly in winter, the WPS seawater intrudes into the nSCS through the Luzon Strait as a branch of Kuroshio, affecting the seawater chemistry, productivity, and the flux of sinking particles in the nSCS (Lui et al., 2018; Lui et al., 2020). Largely due to changes in the wind stress curl, the Kuroshio intrusions intensify during the El Niño years or Pacific Decadal Oscillation (PDO) warm phases and weaken during the La Niña years or PDO cold phases (Wu, 2013; Nan et al., 2015). The intruded Kuroshio had a similar temperature as that of the nSCS. In contrast, the nutrient concentrations of the surface and subsurface WPS seawaters have significantly higher salinities but lower nutrient concentrations than that of the nSCS. Lui et al. (2020) demonstrated that a strong Kuroshio intrusion occurred around 2003–2004 (El Niño event, PDO warm phase). Consequently, nitrates and phosphate concentrations at 100 m depth decreased from as high as about 12 μM and 0.9 μM in 2000–2002 to as low as 2.2 μM

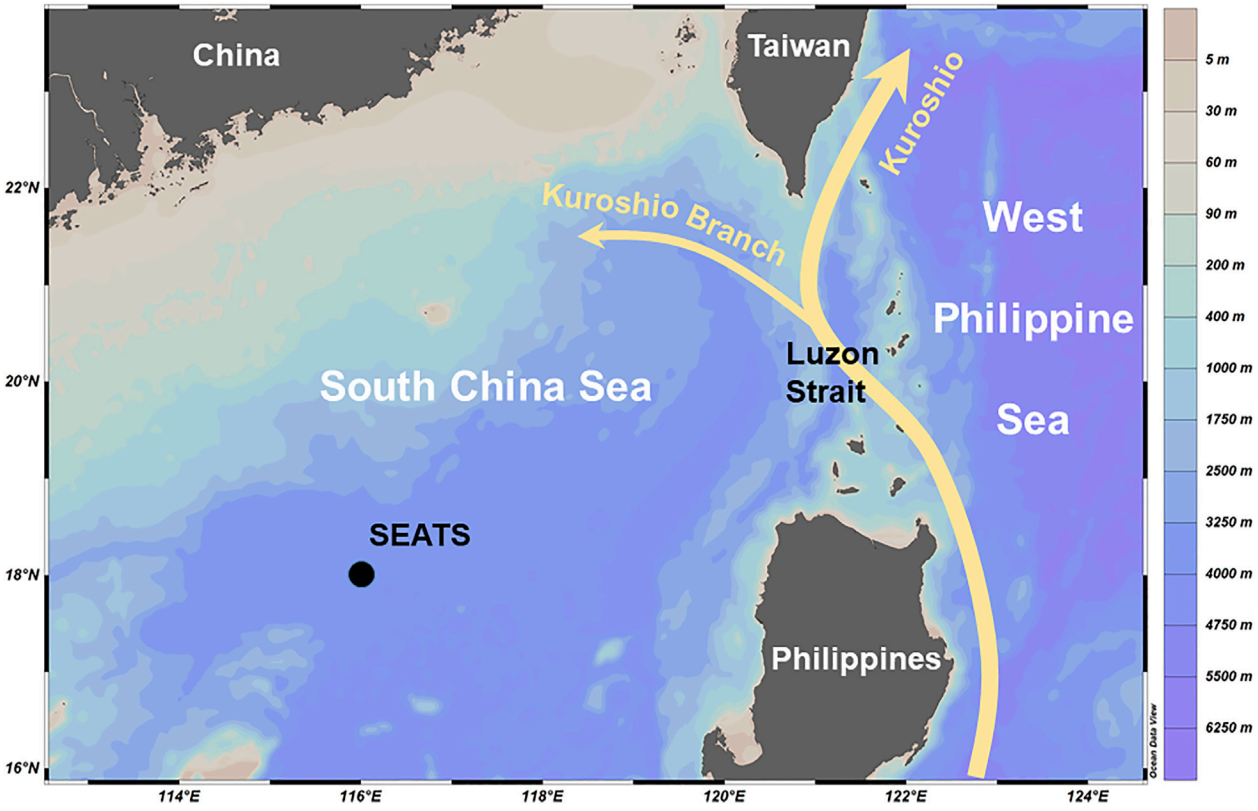

FIGURE 1
Location map for SEATS time-series station and basic hydrology. The curves and arrows show the typical Kuroshio main stream and branch. The map was generated using Ocean Data View 5.0.0. Schlitzer, R., Ocean Data View, https://odv.awi.de, 2018.

and 0.2 μM in 2004, respectively. Since the productivity of the oligotrophic nSCS mainly is controlled by the nutrient inventories, the productivity and the fluxes of sinking particles at the SEATS station also experienced strong interannual oscillations (Tseng et al., 2009b; Wan et al., 2010; Liu et al., 2014; Wong et al., 2015; Lui et al., 2018; Ladigbolu et al., 2020; Lui et al., 2020; Tan et al., 2020).

In this study, trapped foraminifera were collected over the interval spanning from August 2016 to August 2019, a period covering the winter of late 2017 and early 2018 (denoted as 2017/2018; A La Niña event) and 2018/2019 (An El Niño event) according to the monthly Oceanic Niño Index (ONI) from the United States National Oceanic and Atmospheric Administration (NOAA) (https://origin.cpc.ncep.noaa.gov/products/analysis_monitoring/ensostuff/ONI_v5.php). This study aimed to investigate the connection between the time-series of foraminifera fluxes, their species compositions, and regional climatic changes in the deep basin of the nSCS. Relative abundances and shell fluxes of planktonic foraminifera were employed to evaluate the influence of hydrographic setting in the context of the prevailing monsoon system and ENSO.

2 Materials and methods

The collection of sinking particles for this study spanned from September 2013 to August 2019 (moorings SEATS 1–10). Sediment traps were placed at two depths (2,000 m and 3,500 m) with collecting areas and sampling intervals per unit collecting cup of 1 m^2 and 8 days (SEATS 1–3, 6, and 8–10) or 0.05 m^2 and 16 days (SEATS 4, 5, and 7). A complete set of trap mooring contained 24 cups (traps SEATS 1–3, 6, and 8–10 with 1 m^2 collecting area) or 12 cups (traps SEATS 4, 5, and 7 with 0.05 m^2 collecting area) for each depth. The use of a longer collecting interval is to compensate for the decrease of samples collected by the smaller traps. A longer collecting interval, however, generates lower resolution. Before deployment, each cap was filled with brine (0.2 μm filtered *in-situ* seawater with additional NaCl) and $HgCl_2$ with a concentration of 1 g/L for preservation. The cups were stored immediately below 4°C after retrieving the traps. Each trap sample was pre-filtered using a 1 mm × 1 mm pore size opening sieve to remove swimmers and large particles and was split into eight fractions using the Perimatic Premier Pump dispenser and an orbital shaker for further experiments. One fraction was used to determine the total mass flux by the Taiwan

Ocean Research Institute (TORI) of the National Applied Research Laboratories, and one fraction was used to determine the foraminiferal shells in this study. To determine the mass flux, water was filtered through a 0.45 μm pore filter. The filter was then rinsed with deionized water to remove salt. The total mass was weighted after the freeze-drying process was completed. The flux was determined by dividing the total mass by the sample collection interval. The mass flux data used in this study were provided by the TORI. Further detail was provided by Wei et al. (2017) and Lui et al. (2018).

Particle properties were analyzed for total mass flux between August 2013 and August 2019 and for foraminiferal shell flux and its species composition between August 2016 and August 2019. Planktonic foraminifera were examined from four consecutive sets of sediment trap moorings, SEATS 6, 8, 9, and 10, deployed at the SEATS station with a bottom depth of 3,783 m in the nSCS (18°N, 116°E; Figure 1). Samples from mooring SEATS 7 (from 28 April 2017 to 5 November 2017) were not granted due to an insufficient amount of sinking particles by using a small collecting area (0.05 m^2) trap. Specimens were picked from material collected in a sediment trap array deployed from 18 August 2016 to 1 January 2017 (SEATS 6), from 18 November 2017 to 29 May 2018 (SEATS 8), from 11 July 2018 to 19 January 2019 (SEATS 9), and from 28 January 2019 to 8 August 2019 (SEATS 10). Unfortunately, seven intervals from SEATS 6 and collecting cups at the upper level (2000 m) of SEATS 9 were not recovered due to mechanical problems. Species and the original counts are given in the Supplementary Table S1.

The procedures used to process the trap samples followed those of Heussner et al. (1990). Aliquots from each collecting cup were freeze-dried and then soaked in deionized distilled water. Only planktonic foraminifera with shell sizes greater than 212 μm, and not the commonly used 154 μm, were examined to maximize the usefulness of particles collected by sediment traps. A systematic bias existed between our foraminiferal counts and the other studies using shell sizes of >125 μm.

Seawaters at various depths at the SEATS station were sampled using the conductivity, temperature, and pressure unit (the so-called CTD unit) from four cruises in November 2017 (OR1-1184), July 2018 (LGD-T11), August 2019 (LGD-1910), and November 2019 (LGD-1914). [PO_4^{3-}] was analyzed using the nutrient standard provided by Ocean Scientific International Ltd. Chen and Wang (2006) provided information in detail. Using the same research vessel OR1, the temperature, salinity, and fluorescence data of the other two individual cruises (November 2018 and September 2019) were taken to compare with the data of OR1-1184. This study used the level 2 satellite-derived chlorophyll *a* (Chl-a) data measured by moderate resolution imaging spectroradiometers (MODIS) Terra and Aqua with 50 × 50 km^2 area (centered at SEATS, 18°N, 116°E) and 1 km^2 resolution. The monthly (30 days) moving average was adopted to remove daily and monthly fluctuations. Information was provided in detail by Lui et al. (2018). The cross-calibrated multi-platform (CCMP) global wind data, versions 2.0 (1987–2019) and 2.1 (2015–2021), were downloaded from the remote sensing systems (https://www.remss.com/measurements/ccmp/). The spatial and temporal resolutions of the CCMP product are 0.25° × 0.25° and 6 h, respectively. A yearly moving average was applied to filter the seasonal and shorter frequency variations.

3 Results and discussion

3.1 Lunar-like, seasonal and interannual variations of mass and shell fluxes

Figure 2 shows the 2013–2019 monthly smoothed ONI, satellite-derived Chl-a concentration, and total mass flux and the 2016–2019 planktonic foraminifera flux from four sets of moorings. Most of the mass fluxes were around 100 mg m^{-2} day^{-1}, except for the winter months, with 2–3-fold higher fluxes (Figure 2B). Overall, the fluxes at 2,000 m are slightly higher than at 3,500 m, with an average difference of 10.5 ± 54.5 (n = 155) mgm^{-2} day^{-1}. Tan et al. (2020) showed that at a station about 56 km north of the SEATS station, the fluxes of sinking particles between May 2014 and March 2015 were the lowest of 59.7 mg m^{-2} day^{-1} in July 2014 and the highest of 413.2 mg m^{-2} day^{-1} in January 2015 at 1,003 m depth. It is of note that such values had no statistical differences than that of this study but at a deeper depth of 2,000 m, having the lowest of 45.6 mg m^{-2} day^{-1} in August 2014 and the highest of 436.4 mg m^{-2} day^{-1} in February 2015. The slight differences between fluxes at various depths likely were because of fast sinking speed and minimal horizontal particulate transport (Wei et al., 2017; Lui et al., 2018). The fast sinking rate explained one of our observations that although the saturation state of calcite reduced from supersaturation to undersaturation at about 2,500 m in the nSCS (Chen et al., 2006), no additional observable dissolution was found in the shells collected at 3,500 m depth when compared with that at 2,000 m. In this study, larger differences between the fluxes at 2,000 m and 3,500 m mainly occurred in winter, possibly reflecting a better preservative condition for the particulate organic matter from the euphotic zone to before reaching 2,000 m depth in the periods with higher mass fluxes. Generally, the elevated mass fluxes during winter months were consistent with previous deployments reported by Lui et al. (2018). In winter, nutrient inventories in the euphotic zone increase due to enhanced vertical mixing resulting from the strong winter monsoon and seawater cooling. Consequently, productivity and export production increase. The satellite-derived Chl-a data matched well with the mass flux data, supporting that the high and low mass fluxes in winter and summer, respectively, reflect the seasonal changes in the nutrient inventories and productivity in the euphotic zone of the nSCS.

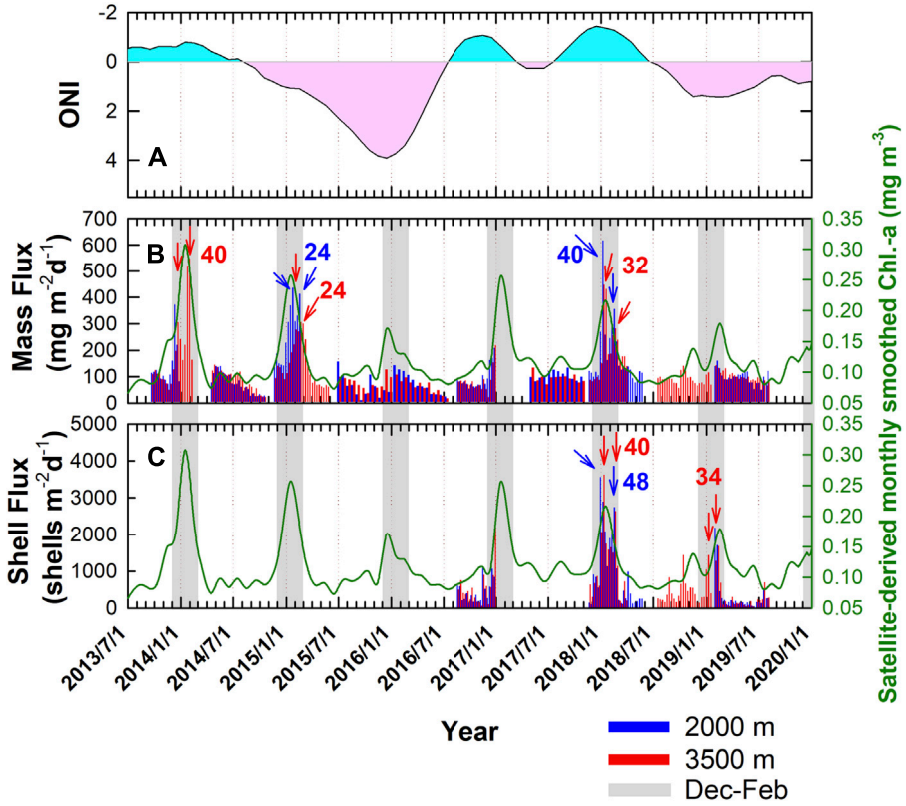

FIGURE 2
Time series of **(A)** ONI (pink and light blue areas refer to positive and negative values, respectively), **(B)** mass, and **(C)** total shell fluxes at 2,000 m (blue) and 3,500 m (red), and **(B and C)** monthly average chlorophyll *a* concentration (green line) at SEATS. Gray bars indicate the periods of December to February. Blue and red arrows indicated the peak values at 2,000 m and 3,500 m depths, respectively. Numbers indicated the time intervals between the arrows (unit: day).

Notably, the extraordinary peaks of the mass fluxes in January 2018 (Figure 2B) showed fluxes 4–6-fold higher than the average value. This extremely high mass flux interval was also manifested in the total planktonic foraminifera shell flux (Figure 2C). Compared with two other years, i.e., 2016 and 2018/2019, total shell fluxes reached almost double peak values in 2017/2018. Similar to the seasonal variations of mass fluxes, the annual high shell fluxes appeared in the winter months (Figure 2C). It is worth mentioning that the shell fluxes are underestimated to a certain extent because the proportion of smaller or juvenile foraminifera with size <212 μm was discounted for their contribution to these seasonal changes. Of note, two observable peaks of mass or shell fluxes usually occurred in winter (arrows shown in Figures 2B and C) between December and January or January and February, having time intervals of 24–40 days for the mass fluxes and 34–48 days for the shell fluxes. Similar periodicities were reported in the Taiwan Strait; shell abundances increased from the lowest at the new moon to their maxima before the full moon (Lin, 2014). Similar cases were also reported in various places, such as the Atlantic Ocean and the Red Sea (Bijma et al., 1990; Venancio et al., 2016). Foraminiferal shell flux below the euphotic layer could be affected by the lunar periodicity, yet the reproduction would be out of the lunar phase (Venancio et al., 2016). Using 4-year trap data at 700 m depth in the northern Gulf of Mexico, Jonkers et al. (2015) showed that the shell fluxes of some foraminiferal species were characterized by some degree of lunar periodicity. The 34–48 days periods found in the deep nSCS were different from the lunar cycle of about 28 days, possibly reflecting the average life span of the collected species (Lin, 2014; Jonkers et al., 2015). The reason for the double peak values remains uncertain. A longer time series data will help to have a better look at the driving mechanisms.

Superimposed on the strong seasonal oscillations of the mass and the shell fluxes are the observable interannual variations. The winter peaks of the mass flux values were the highest in 2017/2018 and the lowest in 2015/2016 and 2018/2019 (Figure 2B). Generally speaking, the interannual variations of the mass and the shell fluxes had similar but opposite patterns to that of the ONI. For instance, the winter peak values gradually decreased

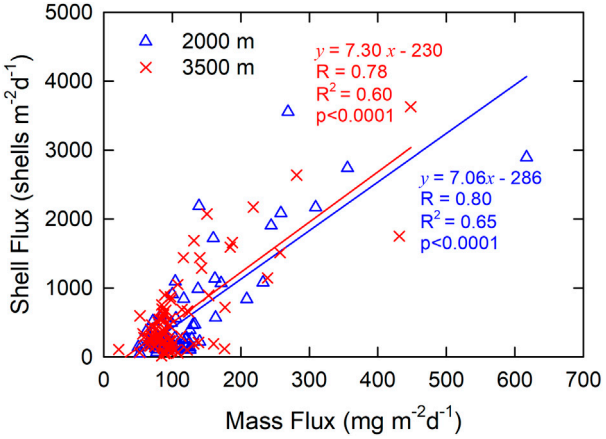

FIGURE 3
Shell vs. mass fluxes at 2,000 m (blue triangle) and 3,500 m (red triangle) between 2016 and 2019 at SEATS station. The lines and equations in blue and red show the linear regression results of data at 2,000 m and 3,500 m, respectively.

from the highest in 2013/2014 to the lowest in 2015/2016 when the ONI gradually changed from the cold phase to the warm phase (Figure 2). Tseng et al. (2009a) showed that the reduced wind speed and the depth of vertical mixing in the El Niño events significantly reduced the nutrient inventories and primary production at the SEATS site. Additionally, the weakened Kuroshio off Luzon Strait during the ENSO warm phase favored the intrusion of Kuroshio into the nSCS (Wu, 2013). Lui et al. (2018) further pointed out the intrusion of the WPS seawater into the nSCS as the Kuroshio branch further decreased the nutrient inventories of the euphotic layer and, hence, the productivity of the nSCS. The well-matched patterns of changes in the time-series data of ONI, mass and shell fluxes, and satellite-derived Chl-a data support the mechanisms mentioned earlier. Lui et al. (2020) demonstrated that the correlation coefficients (R) between the changes in the amount of Kuroshio intrusions and the PDO index from 1999–2016 was 0.58.

Atmospheric dust deposition is a very important source of the sinking particles and metals in the oligotrophic nSCS (Ho et al., 2011; Tan et al., 2020; Liao et al., 2021). At a station about 56 km north of the SEATS station, Tan et al. (2020) showed that carbonate was the major constituent (40%–58% of the mass flux) at a depth of 1,003 m, and lithogenic sources contributed 14%–40% of the mass fluxes. Of note, the mass flux at this site was highly correlated with the carbonate flux, net primary production, and surface seawater temperature, having R values of 0.99, 0.88, and −0.77, respectively. Using the first-order linear regression method, this study showed that the R values between mass and shell fluxes at SEATS have similar but lower values of 0.80 at 2,000 m depth and 0.78 at 3,500 m depth (Figure 3). Based on the coefficient of determination (R^2) values, the result shows that the mass flux predicted 65% and 60% of the variations of the shell fluxes at 2,000 m and 3,500 m depths, respectively, based on the first-order linear regression model. It is worth mentioning that the fluxes of foraminiferal shells counted a small proportion of the mass and carbonate fluxes. The relatively low R^2 values suggest that, in addition to productivity and mass flux, other factors are at play controlling the shell fluxes, such as resuspension, lateral transport, and the life cycle of foraminifera (Lin, 2014; Liu et al., 2014; Jonkers et al., 2015; Ran et al., 2022). Indeed, different species of foraminifera respond differently under various environmental conditions, such as having different seasonal cycles, as discussed below.

3.2 Species composition of sinking foraminiferal shells

A total of 11 common species were identified from the samples. These species include *Globigerinoides ruber, Trilobatus sacculifer, Globigerinella siphonifera, Pulleniatina obliquiloculata, Neogloboquadrina dutertrei, Globorotalia menardii, Globigerina bulloides, O. universa, Globigerinita glutinata. Globigerinella calida,* and *Globigerinoides conglobatus*. Specimens that did not belong to the above species were counted as "others" and were calculated as part of the sum. It is worth mentioning that the "others" counted for just 3.1% ± 3.8% of the total, showing that the 11 species we selected were the dominant ones (See appendix table and Figure 5 for detail). Figure 4 shows the shell fluxes (number of shells m^{-2} day^{-1}) for four major species (20% or higher for the relative abundance with the comparison of the ONI, see Figure 5 for detail) *G. ruber*, *T. sacculifer*, *G. siphonifera*, and *N. dutertrei*. In general, these species showed significant peak values in winter (Figure 4). This is also the case for diatoms in the nSCS that have higher vertical diatom fluxes in winter than in summer, reflecting the enhanced growth of diatoms in winter (Ran et al., 2015). Similar to the elevated total shell fluxes in 2017/2018 (Figure 2C), a pronounced increase in shell flux was also a common feature among the four species shown in Figure 4, particularly the amplitude of multiple increases shown by *N. dutertrei* (Figure 4E). In terms of shell flux, *T. sacculifer* had much higher fluxes than *G. ruber*. In general, these four species had similar lunar-like cycles. A decreasing trend for *G. ruber* occurred from August 2016 to February 2017, making it different from the other species in this period. In the case of *G. ruber*, the differences between the peak values from August 2018 to December 2018 were between 34 and 47 days (Figure 4B), which might reflect an average life span of foraminifera (Lin, 2014; Jonkers et al., 2015).

Figure 5 shows the species composition as relative abundance in a consecutive sequence for the four collection intervals between 2016 and 2019 with the comparison of the ONI. An abrupt increase, from the average relative abundance of 10% to over 60%, of *N. dutertrei* in early 2018 represented the most conspicuous feature of all relative abundances shown in Figure 5. Nevertheless, this distinctive proliferation event was also marked by its multiple

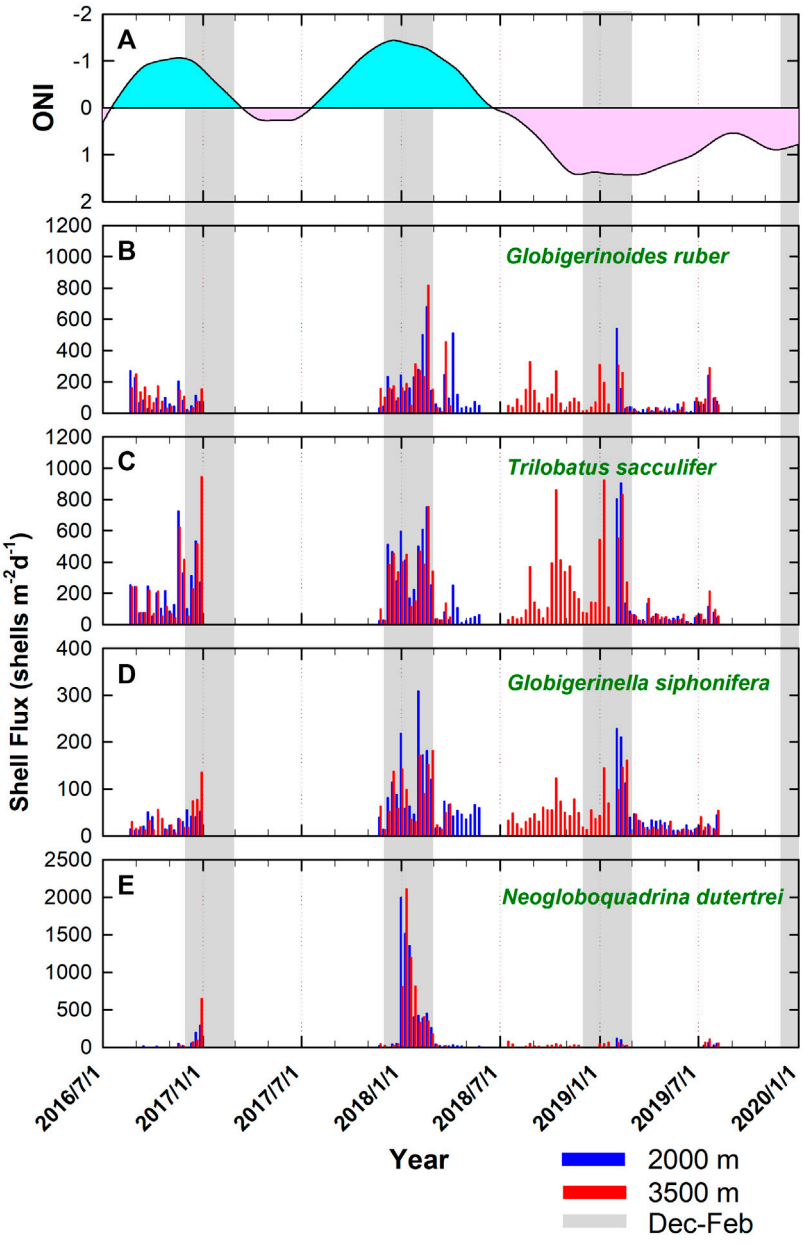

FIGURE 4
Time series of **(A)** ONI (pink and light blue areas refer to positive and negative values, respectively) and annual shell fluxes (numbers of shells m^{-2}·day^{-1}) for **(B)** *Globigerinoides ruber*, **(C)** *Trilobatus sacculifer*, **(D)** *Globigerinella siphonifera*, and **(E)** *Neogloboquadrina dutertrei*. Gray bars indicate the periods of December to January.

increases in shell flux (Figure 4E). The significant peak of *N. dutertrei* lasted for about 1 month (four collection intervals). As a nonspinose species, *N. dutertrei* secrete their shells over a broad range of depths during their ontogenetic cycle (Fairbanks et al., 1980; Fairbanks and Wiebe, 1980; Fairbanks et al., 1982; Bouvier-Soumagnac and Duplessy, 1985). It is regarded as a subsurface-dweller that usually reaches its maximum abundance in the thermocline (Fairbanks et al., 1982; Curry et al., 1983; Ladigbolu et al., 2020). A recent sediment trap study conducted off southwest Hainan Island confined it as a thermocline dweller with its calcification depth at 75–100 m according to stable isotope analysis (Ladigbolu et al., 2020).

The remaining six species, *G. menardii*, *G. bulloides*, *O. universa*, *G. glutinata*, *G. calida*, and *G. conglobatus*, as displayed in Figures 5G–L, were less abundant (<10%) throughout most of the record. Yet, there was an interval characterized by a greater abundance of *O.*

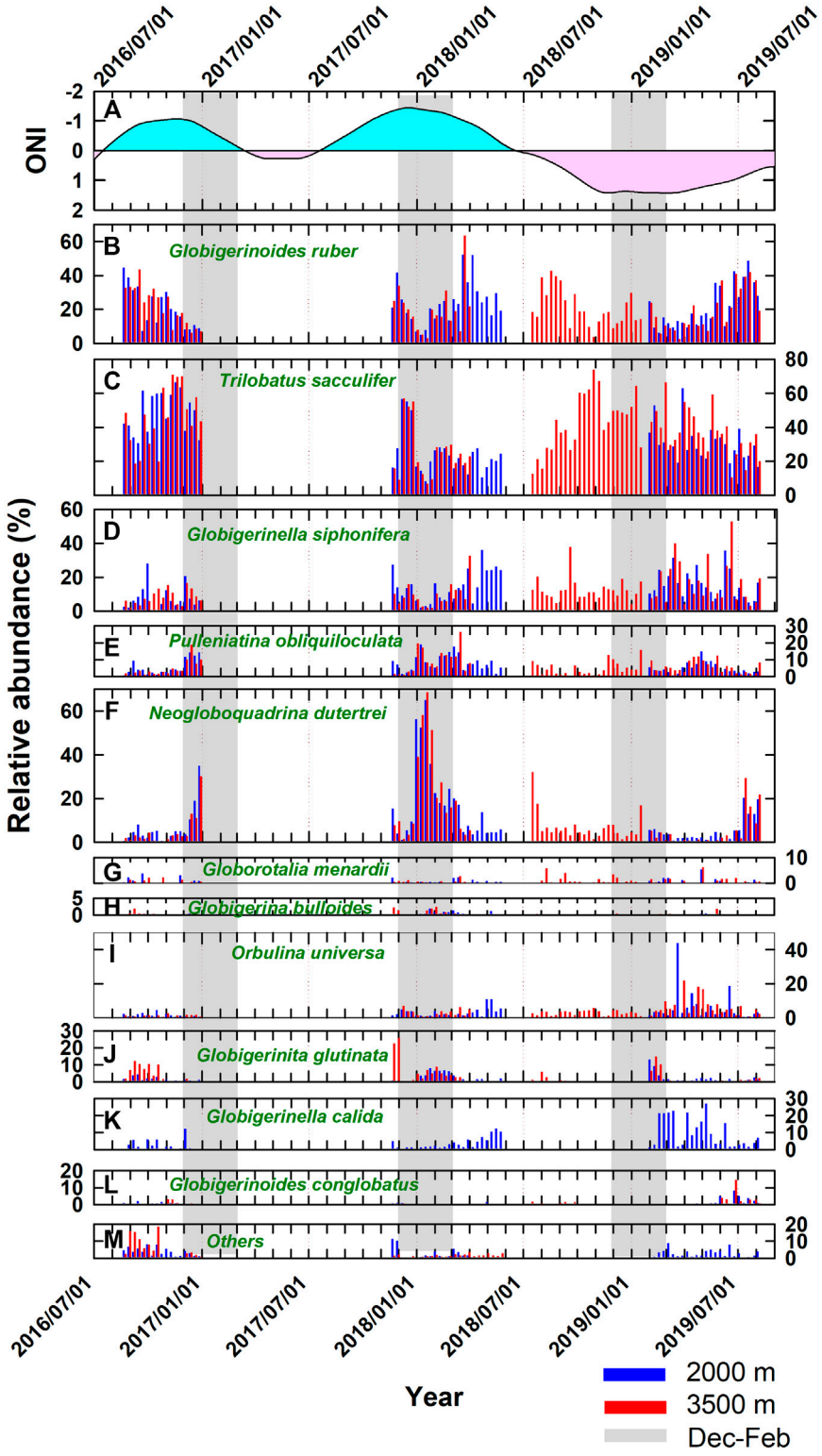

FIGURE 5
Time series of **(A)** ONI (pink and light blue areas refer to positive and negative values, respectively) and relative abundance of **(B–L)** 11 species and **(M)** others for the four collection intervals in a consecutive sequence. Gray bars indicate the periods of December to January.

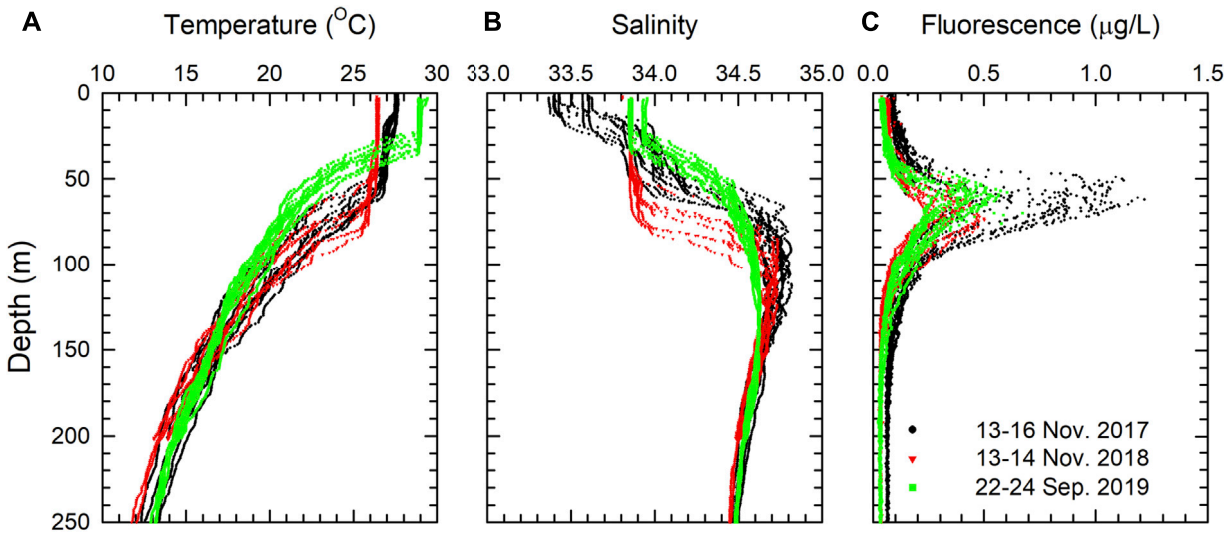

FIGURE 6
Profiles of **(A)** temperature, **(B)** salinity, and **(C)** fluorescence obtained from onboard RV ORI CTD. The casts were conducted during the deployment and recovery of sediment trap moorings near the SEATS site from 13–16 November 2017 (in black), 13–14 November 2018 (in red), and 22–24 September 2019 (in green).

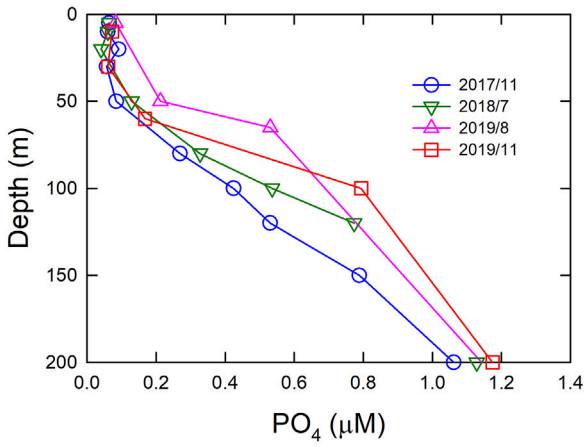

FIGURE 7
Phosphate concentration vs. depth at SEATS between 2017 and 2019.

universa and *G. calida* in the last set of trap mooring (April-June 2019), concurrent with a pronounced low frequency of *N. dutertrei* and total shell fluxes (Figure 2C). An increased flux of *O. universa*, together with *G. siphonifera* and *T. sacculifer*, collected by the weekly to biweekly resolved sediment trap moored in the North Atlantic, indicated a warm, well-stratified surface ocean (Chapman, 2010). This, likely, was not the case in this study as the peaks for *O. universa* and *G. calida* occurred mainly in spring. The abundance of *G. glutinata* obtained by this study might have been underestimated due to its small shell size since foraminifera shells were only examined with a size fraction greater than 212 μm in this study, whereas specimens with shell sizes between 63 and 212 μm were not included. The size fraction contains individual species at their juvenile stage and/or small species in nature. Therefore, the contribution from small shells might have been underrated. Contrary to the abundant *N. dutertrei* related to the aforementioned elevated Chl-a concentrations, the warm months of 2019 featured low *N. dutertrei* and total shell flux but more *O. universa* and *G. calida*. Having the depth of vertical mixing reduced in summer, the surface layer at the SEATS site usually depleted in nutrients, especially nitrate. The increases in *O. universa* and *G. calida* might reflect an oligotrophic condition in this period. This interval was also recognized as a weak phase of El Niño, according to the ONI.

3.3 Physical and chemical forcings of changing nutrient inventories and productivity

To explore the possible forcing responsible for the mass production of *N. dutertrei* preserved in January 2018, profiles of temperature, salinity, and fluorescence concentration retrieved from CTD units are plotted for the upper 250 m in Figure 6. The onboard research vessel CTD casts were conducted during the deployment and recovery of sediment trap moorings near the SEATS site in November 2017, November 2018, and September 2019. The depth of the mixed layer in 2018 was the deepest (up to

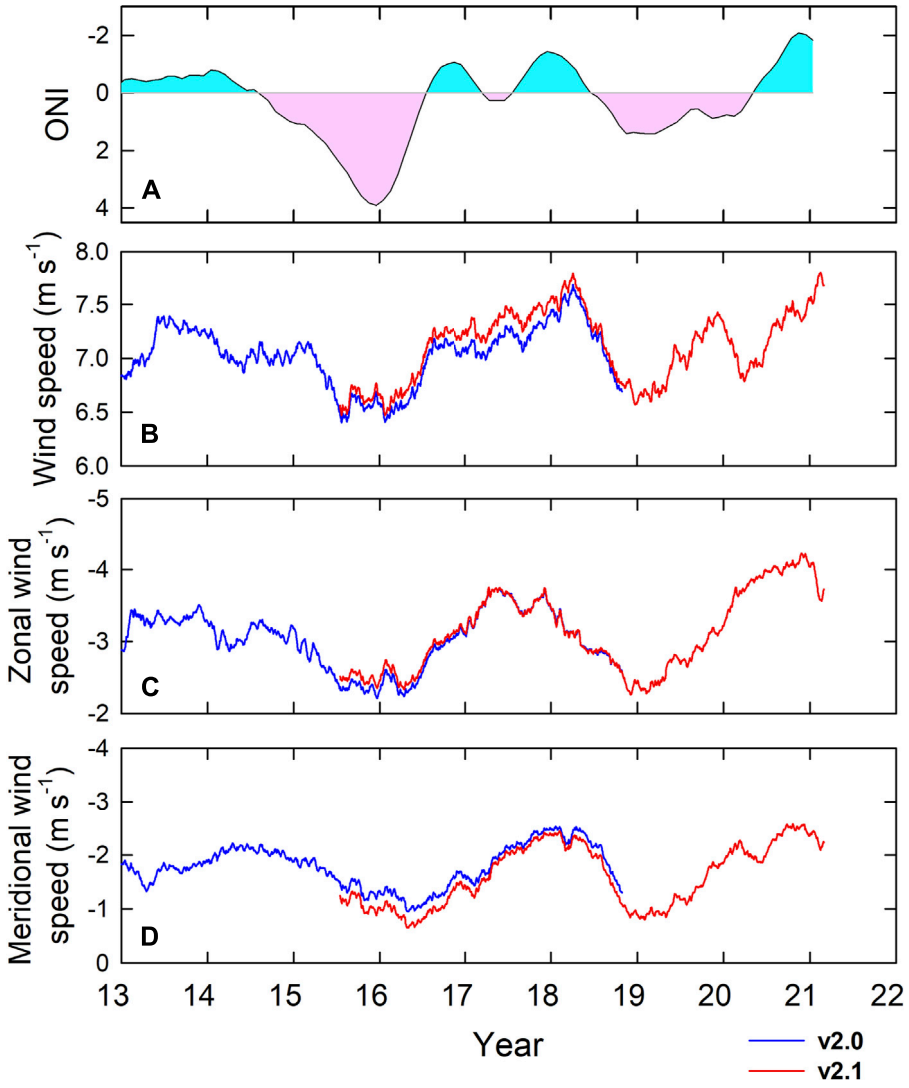

FIGURE 8
Time-series of **(A)** ONI (pink and light blue areas refer to positive and negative values, respectively) and yearly-smoothed satellite-derived **(B)** wind speed, **(C)** zonal wind speed, and **(D)** meridional wind speed at SEATS between 2013 and 2021. The blue and red lines show the v2.0 and v2.1 data, respectively.

80 m), while that in 2019 was the shallowest (30–40 m) according to the profiles of temperature and salinity (Figures 6A and B). Compared with the other surveys, the doubling of fluorescence concentration in 2017 is of special interest (Figure 6C). The increase in fluorescence concentration was concurrent with the 2017/2018 La Niña event, providing a satisfactory condition for the flourish of planktonic foraminifera. Although there were a few weeks apart between the CTD cast peak values of shell flux (13–15 November 2017 vs. January 2018; the sixth collecting cup after deployment), this can be attributed to the transfer of the food chain from phytoplankton to zooplankton, the life span of foraminifera, and the time required for sinking to 2,000 and 3,500 m. A similar situation was observed off south Java; net primary production and foraminiferal flux rates were highest from July to October when the upwelling of upper seawater to the euphotic zone was enhanced by the Southeast monsoon (Mohtadi et al., 2009). In the Gulf of Aqaba of the northern Red Sea, the highest annual planktonic foraminifera flux was found a few days later than the annual surface Chl-a peak based on a 1-year, daily-resolved sediment trap moored at a water depth of 410 m (Chernihovsky et al., 2020). As a result, the accumulation of planktonic foraminifera induced by the spring blooms in the Gulf of Aqaba lasted for a few weeks and accounted for one-third of the total annual planktonic foraminifera flux. In the oligotrophic subtropical gyre of the South Indian Ocean, the average total mass flux was just 9.8 ± 3.7 mg m^{-2} day^{-1} between 2,000 and

3,000 m depths. In general, the net primary production followed the temporal trends of the wind speed, as higher wind speed referred to deeper mixed layer depth and hence higher nutrient inventories in the euphotic zone. In oligotrophic oceans, the amounts of nutrients entering the euphotic zone control the productivity, export production, and the mass and foraminiferal fluxes.

Previous studies showed that, largely due to changes in the wind stress curl, the ENSO warm phases (positive ONI) intensified the amount of the intrusion of WPS seawater to the nSCS, and vice versa in the cold phases (negative ONI) (Tseng et al., 2009a; Wu, 2013; Nan et al., 2015; Lui et al., 2018; Lui et al., 2020). Generally speaking, the increase in the WPS water intrusion reduces the nutrient inventories and productivity in the nSCS (Wu, 2013; Lui et al., 2018; Lui et al., 2020). This is because the nutrients of the WPS seawater were significantly lower than that of the nSCS in the subsurface layer. Such a result is similar to the case in the Western Pacific Warm Pool; productivity and the mass fluxes decreased in the central and eastern Western Pacific Warm Pool when a warm but low nutrient water mass overlayed the nutrient-rich cold water at the surface layer (Kawahata et al., 2000). Our observation showed that the phosphate concentration gradually increased in the upper layer of seawater (0–200 m, Figure 7) between November 2017 and November 2019, when the ONI showed an increasing trend. Meanwhile, both mass fluxes and satellite-derived Chl-a concentrations in the winter of 2017/2018 were high and low in the winter of 2018/2019. It is of note that although the nutrient concentration in 2019 was the highest at 100 and 200 m depths since November 2017, both satellite-derived Chl-a and mass flux were the second-lowest in the wintertime of 2018/2019. Such a result is similar to that of 2016 and can be attributed to the reduced vertical mixing under a reduction in wind speed and discuss as follows.

In the SCS, our result shows that the yearly-smoothed wind speeds (Figure 8B) and their zonal (Figure 8C) and meridional (Figure 8D) components were relatively weak in the warm phases of ENSO when compared with the ENSO cold phases (Figure 8A). During the cold phases in our study period, the wind speeds in the winter of 2017/2018 and 2020/2021 were the highest at 7.8 ms^{-1}. Consequently, Chl-a concentrations and the mass and shell fluxes were high (Figures 2B and C). In contrast, during the ENSO warm phases, the wind speeds in the winter of 2015/2016 and 2018/2019 were the lowest (6.5 ms^{-1}) and second lowest (6.6 ms^{-1}), respectively, in our study period (Figure 8). Consequently, the Chl-a concentration and the mass and shell fluxes were also the lowest (Figures 2B and C). Such results imply that an 15%–17% reduction in wind speed might lead to a several-fold decrease in the mass and foraminiferal shell fluxes and *vice versa*.

4 Conclusion

Time-series of sinking particle records received by the sediment trap moorings deployed in the nSCS between September 2013 and August 2019 were examined to reveal the influence of climatic events in this study. In addition to total mass fluxes collected at water depths of 2,000 and 3,500 m, planktonic foraminiferal census between August 2016 and August 2019 obtained from traps was investigated to provide insight into the responses of zooplanktons to hydrographic changes. Basically, the temporal changes of species compositions of planktonic foraminifera mimicked the surface productivity through the research interval. Lunar-like but longer periodicities in mass and shell fluxes were characterized, which might reflect an average life span of various foraminifera species. The changes in climate conditions during ENSO cold phase resulted in a 2–3-fold increase in the sinking particles and the planktonic foraminifera shell fluxes. The SCS study shows that the mass and the foraminiferal shell fluxes are controlled by the nutrient inventories in the euphotic zone. Changes in the strength of the monsoon are critical factors for the changes in nutrient inventories. Using the fluxes of foraminiferal shells as an example, this study provides insight into how climatic change might cause significant changes in the biological pump of the ocean.

Data availability statement

The original contributions presented in the study are included in the article/Supplementary Material; further inquiries can be directed to the corresponding author.

Author contributions

The foraminifera analysis was performed by HLL and TCL, the hydrography and nutrient data analysis was performed by HKL and the satellite-derived wind data analysis was performed by YLW.

Funding

This research was funded by the Ministry of Science and Technology of Taiwan (MOST 108-2611-M-110-012, MOST 110-2611-M-110-024- and MOST 111-2611-M-110-025-).

Acknowledgments

The authors thank TORI for providing the mass flux data and the trap samples. The authors also thank Dr. Jen-Hua Tai at the Academia Sinica, who led the cruises and provided the CTD data in November 2017 and September 2019. The authors also thank the PIs of the cruises and the captain and crew of R/V *Ocean Researchers I*, *III*, and *Legend*. Two reviewers provided detailed and constructive comments, which helped strengthen the manuscript.

Conflict of interest

The authors declare that the research was conducted in the absence of any commercial or financial relationships that could be construed as a potential conflict of interest.

Publisher's note

All claims expressed in this article are solely those of the authors and do not necessarily represent those of their affiliated organizations, or those of the publisher, the editors, and the reviewers. Any product that may be evaluated in this article, or claim that may be made by its manufacturer, is not guaranteed or endorsed by the publisher.

Supplementary material

The Supplementary Material for this article can be found online at: https://www.frontiersin.org/articles/10.3389/10.3389/feart.2022.928115/full#supplementary-material

References

An, B., Li, T., Liu, J., Sun, H., and Chang, F. (2018). Spatial distribution and controlling factors of planktonic foraminifera in the modern Western Pacific. *Quat. Int.* 468, 14–23. doi:10.1016/j.quaint.2018.01.003

Bemis, B. E., Spero, H. J., Lea, D. W., and Bijma, J. (2000). Temperature influence on the carbon isotopic composition of Globigerina bulloides and Orbulina universa (planktonic foraminifera). *Mar. Micropaleontol.* 38 (3-4), 213–228. doi:10.1016/s0377-8398(00)00006-2

Bertlich, J., Nürnberg, D., Hathorne, E. C., de Nooijer, L. J., Mezger, E. M., Kienast, M., et al. (2018). Salinity control on Na incorporation into calcite tests of the planktonic foraminifera <i>Trilobatus sacculifer</i> – evidence from culture experiments and surface sediments. *Biogeosciences* 15 (20), 5991–6018. doi:10.5194/bg-15-5991-2018

Bijma, J., Erez, J., and Hemleben, C. (1990). Lunar and semi-lunar reproductive cycles in some spinose planktonic foraminifers. *J. Foraminifer. Res.* 20, 117–127. doi:10.2113/gsjfr.20.2.117

Bijma, J., Spero, H., and Lea, D. (1999). "Reassessing foraminiferal stable isotope geochemistry: Impact of the oceanic carbonate system (experimental results)," in *Use of proxies in paleoceanography* (Germany: Springer), 489–512.

Black, D. E., Thunell, R. C., and Tappa, E. J. (2001). Planktonic foraminiferal response to the 1997–1998 El Niño: A sediment-trap record from the santa barbara basin. *Geol.* 29 (12), 1075–1078. doi:10.1130/0091-7613(2001)029<1075:pfrtte>2.0.co;2

Bouvier-Soumagnac, Y., and Duplessy, J.-C. (1985). Carbon and oxygen isotopic composition of planktonic foraminifera from laboratory culture, plankton tows and Recent sediment; implications for the reconstruction of paleoclimatic conditions and of the global carbon cycle. *J. Foraminifer. Res.* 15 (4), 302–320. doi:10.2113/gsjfr.15.4.302

Chapman, M. R. (2010). Seasonal production patterns of planktonic foraminifera in the NE Atlantic Ocean: Implications for paleotemperature and hydrographic reconstructions. *Paleoceanography* 25 (1), PA1101. doi:10.1029/2008PA001708

Chen, C.-T. A., and Wang, S.-L. (2006). A salinity front in the southern East China Sea separating the Chinese coastal and Taiwan Strait waters from Kuroshio waters. *Cont. Shelf Res.* 26 (14), 1636–1653. doi:10.1016/j.csr.2006.05.003

Chen, C.-T. A., Yeh, Y.-T., Yanagi, T., Bai, Y., He, X., and Huang, T.-H. (2016). The tug-of-war between the west Philippine Sea and south China sea tropical waters and intermediate waters in the okinawa trough. *J. Geophys. Res. Oceans* 121 (3), 1736–1754. doi:10.1002/2015JC011274

Chen, C. T. A., Wang, S. L., Chou, W. C., and Sheu, D. D. (2006). Carbonate chemistry and projected future changes in pH and $CaCO_3$ saturation state of the South China Sea. *Mar. Chem.* 101 (3), 277–305. doi:10.1016/j.marchem.2006.01.007

Chernihovsky, N., Almogi-Labin, A., Kienast, S. S., and Torfstein, A. (2020). The daily resolved temperature dependence and structure of planktonic foraminifera blooms. *Sci. Rep.* 10 (1), 17456. doi:10.1038/s41598-020-74342-z

Chou, W.-C., Sheu, D. D.-D., Chen, C.-T. A., Wang, S.-L., and Tseng, C.-M. (2005). Seasonal variability of carbon chemistry at the SEATS site, northern South China sea between 2002 and 2003. *Terr. Atmos. Ocean. Sci.* 16 (2), 445–465. doi:10.3319/tao.2005.16.2.445(o)

Curry, W. B., Thunell, R. C., and Honjo, S. (1983). Seasonal changes in the isotopic composition of planktonic foraminifera collected in Panama Basin sediment traps. *Earth Planet. Sci. Lett.* 64 (1), 33–43. doi:10.1016/0012-821X(83)90050-X

Du, S. H., Islam, G. M. A., Xiang, R., and Yang, X. L. (2021). The dust deposition process and biogeochemical impacts in the northern South China Sea. *Asia. Pac. J. Atmos. Sci.* 57 (1), 77–87. doi:10.1007/s13143-019-00171-4

Duhamel, M., Colin, C., Revel, M., Siani, G., Dapoigny, A., Douville, E., et al. (2020). Variations in eastern Mediterranean hydrology during the last climatic cycle as inferred from neodymium isotopes in foraminifera. *Quat. Sci. Rev.* 237, 106306. doi:10.1016/j.quascirev.2020.106306

Fairbanks, R. G., Sverdlove, M., Free, R., Wiebe, P. H., and Bé, A. W. H. (1982). Vertical distribution and isotopic fractionation of living planktonic foraminifera from the Panama Basin. *Nature* 298 (5877), 841–844. doi:10.1038/298841a0

Fairbanks, R. G., Wiebe, P. H., and Bé, A. W. H. (1980). Vertical distribution and isotopic composition of living planktonic foraminifera in the Western North Atlantic. *Science* 207 (4426), 61–63. doi:10.1126/science.207.4426.61

Fairbanks, R. G., and Wiebe, P. H. (1980). Foraminifera and chlorophyll maximum: Vertical distribution, seasonal succession, and paleoceanographic significance. *Science* 209(4464), 1524–1526. doi:10.1126/science.209.4464.1524

Gussone, N., Eisenhauer, A., Heuser, A., Dietzel, M., Bock, B., Böhm, F., et al. (2003). Model for kinetic effects on calcium isotope fractionation (δ44Ca) in inorganic aragonite and cultured planktonic foraminifera. *Geochimica Cosmochimica Acta* 67 (7), 1375–1382. doi:10.1016/S0016-7037(02)01296-6

Heussner, S., Ratti, C., and Carbonne, J. (1990). The PPS 3 time-series sediment trap and the trap sample processing techniques used during the ECOMARGE experiment. *Cont. Shelf Res.* 10 (9), 943–958. doi:10.1016/0278-4343(90)90069-X

Ho, T.-Y., Chou, W.-C., Lin, H.-L., and Sheu, D. D. (2011). Trace metal cycling in the deep water of the South China Sea: The composition, sources, and fluxes of sinking particles. *Limnol. Oceanogr.* 56 (4), 1225–1243. doi:10.4319/lo.2011.56.4.1225

Holland, K., Branson, O., Haynes, L. L., Hönisch, B., Allen, K. A., Russell, A. D., et al. (2020). Constraining multiple controls on planktic foraminifera Mg/Ca. *Geochimica Cosmochimica Acta* 273, 116–136. doi:10.1016/j.gca.2020.01.015

Hönisch, B., Bijma, J., Russell, A. D., Spero, H. J., Palmer, M. R., Zeebe, R. E., et al. (2003). The influence of symbiont photosynthesis on the boron isotopic composition of foraminifera shells. *Mar. Micropaleontol.* 49 (1-2), 87–96. doi:10.1016/s0377-8398(03)00030-6

Jonkers, L., Reynolds, C. E., Richey, J., and Hall, I. R. (2015). Lunar periodicity in the shell flux of planktonic foraminifera in the Gulf of Mexico. *Biogeosciences* 12 (10), 3061–3070. doi:10.5194/bg-12-3061-2015

Kawahata, H., Suzuki, A., and Ohta, H. (2000). Export fluxes in the western pacific warm Pool. *Deep Sea Res. Part I Oceanogr. Res. Pap.* 47 (11), 2061–2091. doi:10.1016/S0967-0637(00)00025-X

Kipp, N. G., Cune, R. M., and Hays, J. D. (1976). "New transfer function for estimating past sea-surface conditions from sea-bed distribution of planktonic foraminiferal assemblages in the North Atlantic," in *Investigation of late quaternary paleoceanography and paleoclimatology* (Boulder: Geological Society of America).

Kuroyanagi, A., and Kawahata, H. (2004). Vertical distribution of living planktonic foraminifera in the seas around Japan. *Mar. Micropaleontol.* 53 (1-2), 173–196. doi:10.1016/j.marmicro.2004.06.001

Ladigbolu, I. A., Li, H. L., Li, B. H., Wiesner, M. G., Zhang, J. J., Sun, L., et al. (2020). Calcification depths and temperatures of planktonic foraminifera off southwest Hainan Island and their paleoceanographic implications. *Mar. Micropaleontol.* 158 (2), 101878. doi:10.1016/j.marmicro.2020.101878

Liao, W.-H., Takano, S., Tian, H.-A., Chen, H.-Y., Sohrin, Y., and Ho, T.-Y. (2021). Zn elemental and isotopic features in sinking particles of the South China Sea: Implications for its sources and sinks. *Geochimica Cosmochimica Acta* 314, 68–84. doi:10.1016/j.gca.2021.09.013

Lin, H.-L., and Hsieh, H.-Y. (2007). Seasonal variations of modern planktonic foraminifera in the South China Sea. *Deep Sea Res. Part II Top. Stud. Oceanogr.* 54 (14-15), 1634–1644. doi:10.1016/j.dsr2.2007.05.007

Lin, H.-L., Sheu, D. D.-D., Yang, Y., Chou, W.-C., and Hung, G.-W. (2011). Stable isotopes in modern planktonic foraminifera: Sediment trap and plankton tow results from the South China Sea. *Mar. Micropaleontol.* 79 (1-2), 15–23. doi:10.1016/j.marmicro.2010.12.002

Lin, H.-L. (2014). The seasonal succession of modern planktonic foraminifera: Sediment traps observations from southwest Taiwan waters. *Cont. Shelf Res.* 84, 13–22. doi:10.1016/j.csr.2014.04.020

Liu, J., Clift, P. D., Yan, W., Chen, Z., Chen, H., Xiang, R., et al. (2014). Modern transport and deposition of settling particles in the northern South China Sea: Sediment trap evidence adjacent to Xisha Trough. *Deep Sea Res. Part I Oceanogr. Res. Pap.* 93, 145–155. doi:10.1016/j.dsr.2014.08.005

Liu, K. K., Wang, L. W., Dai, M., Tseng, C. M., Yang, Y., Sui, C. H., et al. (2013). Inter-annual variation of chlorophyll in the northern South China Sea observed at the SEATS Station and its asymmetric responses to climate oscillation. *Biogeosciences* 10 (11), 7449–7462. doi:10.5194/bg-10-7449-2013

Lui, H. K., Chen, C. T. A., Hou, W. P., Liau, J. M., Chou, W. C., Wang, Y. L., et al. (2020). Intrusion of Kuroshio helps to diminish coastal hypoxia in the coast of northern South China Sea. *Front. Mar. Sci.* 7, 565952. doi:10.3389/fmars.2020.565952

Lui, H. K., Chen, K. Y., Chen, C. T. A., Wang, B. S., Lin, H. L., Ho, S. H., et al. (2018). Physical forcing-driven productivity and sediment flux to the deep basin of northern South China sea: A decadal time series study. *Sustainability* 10 (4), 971. doi:10.3390/su10040971

Mathien-Blard, E., and Bassinot, F. (2009). Salinity bias on the foraminifera Mg/Ca thermometry: Correction procedure and implications for past ocean hydrographic reconstructions. *Geochem. Geophys. Geosyst.* 10 (12), Q12011. doi:10.1029/2008GC002353

Mezger, E. M., de Nooijer, L. J., Boer, W., Brummer, G. J. A., and Reichart, G. J. (2016). Salinity controls on Na incorporation in Red Sea planktonic foraminifera. *Paleoceanography* 31 (12), 1562–1582. doi:10.1002/2016PA003052

Mezger, E. M., de Nooijer, L. J., Siccha, M., Brummer, G.-J. A., Kucera, M., and Reichart, G.-J. (2018). Taphonomic and ontogenetic effects on Na/Ca and Mg/Ca in spinose planktonic foraminifera from the Red Sea. *Geochem. Geophys. Geosyst.* 19 (11), 4174–4194. doi:10.1029/2018GC007852

Mohtadi, M., Steinke, S., Groeneveld, J., Fink, H. G., Rixen, T., Hebbeln, D., et al. (2009). Low-latitude control on seasonal and interannual changes in planktonic foraminiferal flux and shell geochemistry off south Java: A sediment trap study. *Paleoceanography* 24 (1), PA1201. doi:10.1029/2008PA001636

Mulitza, S., Boltovskoy, D., Donner, B., Meggers, H., Paul, A., and Wefer, G. (2003). Temperature:δ18O relationships of planktonic foraminifera collected from surface waters. *Palaeogeogr. Palaeoclimatol. Palaeoecol.* 202 (1), 143–152. doi:10.1016/S0031-0182(03)00633-3

Nan, F., Xue, H., Chai, F., Wang, D., Yu, F., Shi, M., et al. (2013). Weakening of the Kuroshio intrusion into the South China Sea over the past two decades. *J. Clim.* 26 (20), 8097–8110. doi:10.1175/jcli-d-12-00315.1

Nan, F., Xue, H., and Yu, F. (2015). Kuroshio intrusion into the South China sea: A review. *Prog. Oceanogr.* 137, 314–333. doi:10.1016/j.pocean.2014.05.012

Niebler, H. S., and Gersonde, R. (1998). A planktic foraminiferal transfer function for the southern South Atlantic Ocean. *Mar. Micropaleontol.* 34 (3), 213–234. doi:10.1016/S0377-8398(98)00009-7

Nürnberg, D., Müller, A., and Schneider, R. R. (2000). Paleo-sea surface temperature calculations in the equatorial east atlantic from Mg/Ca ratios in planktic foraminifera: A comparison to sea surface temperature estimates from U37K′, oxygen isotopes, and foraminiferal transfer function. *Paleoceanography* 15 (1), 124–134. doi:10.1029/1999PA000370

Pogge von Strandmann, P. A. E. (2008). Precise magnesium isotope measurements in core top planktic and benthic foraminifera. *Geochem. Geophys. Geosyst.* 9 (12), G12015. doi:10.1029/2008GC002209

Rae, J. W. B., Foster, G. L., Schmidt, D. N., and Elliott, T. (2011). Boron isotopes and B/Ca in benthic foraminifera: Proxies for the deep ocean carbonate system. *Earth Planet. Sci. Lett.* 302 (3), 403–413. doi:10.1016/j.epsl.2010.12.034

Ran, L., Chen, J., Wiesner, M. G., Ling, Z., Lahajnar, N., Yang, Z., et al. (2015). Variability in the abundance and species composition of diatoms in sinking particles in the northern South China Sea: Results from time-series moored sediment traps. *Deep Sea Res. Part II Top. Stud. Oceanogr.* 122, 15–24. doi:10.1016/j.dsr2.2015.07.004

Ran, L. H., Ma, W. T., Wiesner, M. G., Wang, Y. T., Chen, J. F., Zhang, L. L., et al. (2022). Sediment resuspension as a major contributor to sinking particles in the northwestern south China sea: Evidence from observations and modeling. *Front. Mar. Sci.* 9, 819340. doi:10.3389/fmars.2022.819340

Ravelo, A. C., and Fairbanks, R. G. (1992). Oxygen isotopic composition of multiple species of planktonic foraminifera: Recorders of the modern photic zone temperature gradient. *Paleoceanography* 7 (6), 815–831. doi:10.1029/92pa02092

Ren, H., Chen, Y.-C., Wang, X. T., Wong, G. T. F., Cohen, A. L., DeCarlo, T. M., et al. (2017). 21st-century rise in anthropogenic nitrogen deposition on a remote coral reef. *Science* 356(6339), 749–752. doi:10.1126/science.aal3869

Rosenthal, Y., Perron-Cashman, S., Lear, C. H., Bard, E., Barker, S., Billups, K., et al. (2004). Interlaboratory comparison study of Mg/Ca and Sr/Ca measurements in planktonic foraminifera for paleoceanographic research. *Geochem. Geophys. Geosyst.* 5 (4), Q04D09. doi:10.1029/2003GC000650

Russell, A. D., Hönisch, B., Spero, H. J., and Lea, D. W. (2004). Effects of seawater carbonate ion concentration and temperature on shell U, Mg, and Sr in cultured planktonic foraminifera. *Geochimica Cosmochimica Acta* 68 (21), 4347–4361. doi:10.1016/j.gca.2004.03.013

Sagawa, T., Kuroyanagi, A., Irino, T., Kuwae, M., and Kawahata, H. (2013). Seasonal variations in planktonic foraminiferal flux and oxygen isotopic composition in the Western North Pacific: Implications for paleoceanographic reconstruction. *Mar. Micropaleontol.* 100, 11–20. doi:10.1016/j.marmicro.2013.03.013

Sanyal, A., Hemming, N., Broecker, W., Lea, D. W., Spero, H. J., and Hanson, G. N. (1996). Oceanic pH control on the boron isotopic composition of foraminifera: Evidence from culture experiments. *Paleoceanography* 11 (5), 513–517. doi:10.1029/96pa01858

Spero, H. J., Bijma, J., Lea, D. W., and Bemis, B. E. (1997). Effect of seawater carbonate concentration on foraminiferal carbon and oxygen isotopes. *Nature* 390 (6659), 497–500. doi:10.1038/37333

Spero, H. J. (1992). Do planktic foraminifera accurately record shifts in the carbon isotopic composition of seawater ΣCO2? *Mar. Micropaleontol.* 19 (4), 275–285. doi:10.1016/0377-8398(92)90033-g

Spero, H. J., and Lea, D. W. (1996). Experimental determination of stable isotope variability in Globigerina bulloides: Implications for paleoceanographic reconstructions. *Mar. Micropaleontol.* 28 (3), 231–246. doi:10.1016/0377-8398(96)00003-5

Spero, H. J., and Lea, D. W. (1993). Intraspecific stable isotope variability in the planktic foraminiferaGlobigerinoides sacculifer: Results from laboratory experiments. *Mar. Micropaleontol.* 22 (3), 221–234. doi:10.1016/0377-8398(93)90045-Y

Tan, S., Zhang, J., Li, H., Sun, L., Wu, Z., Wiesner, M. G., et al. (2020). Deep ocean particle flux in the northern South China Sea: Variability on intra-seasonal to seasonal timescales. *Front. Earth Sci. (Lausanne).* 8, 74. doi:10.3389/feart.2020.00074

Tedesco, K. A., and Thunell, R. C. (2003). Seasonal and interannual variations in planktonic foraminiferal flux and assemblage composition in the Cariaco Basin, Venezuela. *J. Foraminifer. Res.* 33 (3), 192–210. doi:10.2113/33.3.192

Tseng, C. M., Gong, G. C., Wang, L. W., Liu, K. K., and Yang, Y. (2009a). Anomalous biogeochemical conditions in the northern South China Sea during the El-Niño events between 1997 and 2003. *Geophys. Res. Lett.* 36 (14), L14611. doi:10.1029/2009gl038252

Tseng, C. M., Liu, K. K., Wang, L. W., and Gong, G. C. (2009b). Anomalous hydrographic and biological conditions in the northern South China Sea during the 1997–1998 El Niño and comparisons with the equatorial Pacific. *Deep Sea Res. Part I Oceanogr. Res. Pap.* 56 (12), 2129–2143. doi:10.1016/j.dsr.2009.09.004

Tseng, C. M., Wong, G. T., Lin, I. I., Wu, C. R., and Liu, K. K. (2005). A unique seasonal pattern in phytoplankton biomass in low-latitude waters in the South China Sea. *Geophys. Res. Lett.* 32 (8), L08608. doi:10.1029/2004gl022111

Venancio, I. M., Franco, D., Belem, A. L., Mulitza, S., Siccha, M., Albuquerque, A. L. S., et al. (2016). Planktonic foraminifera shell fluxes from a weekly resolved sediment trap record in the southwestern Atlantic: Evidence for synchronized reproduction. *Mar. Micropaleontol.* 125, 25–35. doi:10.1016/j.marmicro.2016.03.003

Wan, S., Jian, Z., Cheng, X., Qiao, P., and Wang, R. (2010). Seasonal variations in planktonic foraminiferal flux and the chemical properties of their shells in the southern South China Sea. *Sci. China Earth Sci.* 53 (8), 1176–1187. doi:10.1007/s11430-010-4039-3

Wei, C. L., Chia, C. Y., Chou, W. C., and Lee, W. H. (2017). Sinking fluxes of (210) Pb and (210)Po in the deep basin of the northern South China Sea. *J. Environ. Radioact.* 174, 45–53. doi:10.1016/j.jenvrad.2016.05.026

Wong, G. T. F., Pan, X., Li, K. Y., Shiah, F. K., Ho, T. Y., and Guo, X. (2015). Hydrography and nutrient dynamics in the northern South China sea shelf-sea (NoSoCS). *Deep Sea Res. Part II Top. Stud. Oceanogr.* 117, 23–40. doi:10.1016/j.dsr2.2015.02.023

Wong, G. T., Ku, T.-L., Mulholland, M., Tseng, C.-M., and Wang, D.-P. (2007). The SouthEast Asian time-series study (SEATS) and the biogeochemistry of the South China sea—an overview. *Deep Sea Res. Part II Top. Stud. Oceanogr.* 54 (14-15), 1434–1447. doi:10.1016/j.dsr2.2007.05.012

Wu, C.-R. (2013). Interannual modulation of the pacific decadal oscillation (PDO) on the low-latitude Western north pacific. *Prog. Oceanogr.* 110, 49–58. doi:10.1016/j.pocean.2012.12.001

Wu, G., and Zhang, Y. (1998). Tibetan plateau forcing and the timing of the monsoon onset over south Asia and the South China sea. *Mon. Weather Rev.* 126 (4), 913–927. doi:10.1175/1520-0493(1998)126<0913:tpfatt>2.0.co;2

Wu, Q., Colin, C., Liu, Z., Thil, F., Dubois-Dauphin, Q., Frank, N., et al. (2015). Neodymium isotopic composition in foraminifera and authigenic phases of the South China Sea sediments: Implications for the hydrology of the North Pacific Ocean over the past 25 kyr. *Geochem. Geophys. Geosyst.* 16 (11), 3883–3904. doi:10.1002/2015GC005871

Yu, J., Elderfield, H., and Hönisch, B. (2007). B/Ca in planktonic foraminifera as a proxy for surface seawater pH. *Paleoceanography* 22 (2), PA2202. doi:10.1029/2006PA001347